PWM Regenerative Rectifiers: State of the Art

J. Rodríguez, *Senior Member, IEEE,* J. Dixon, J. Espinoza, *Member, IEEE,* and P. Lezana.

Abstract— **New regulations impose more stringent limits to current harmonics injected by power converters, what is achieved with Pulse Width Modulated (PWM) rectifiers. In addition several applications demand the capability of power regeneration to the power supply.**
This paper presents the state of the art in the field of regenerative rectifiers with reduced input harmonics and improved power factor.
Topologies for single and three-phase power supply are considered with their corresponding control strategies.
Special attention is given to the application of voltage and current source PWM rectifiers in different processes with a power range from a few kilowatts up to several megawatts.
This paper shows that PWM regenerative rectifiers are a highly developed and mature technology with a wide industrial acceptance.

Index Terms— **Power electronics, regeneration, rectifier, high power factor.**

I. INTRODUCTION

THE AC-DC conversion is used increasingly in a wide diversity of applications: power supply for microelectronics, household-electric appliances , electronic ballast, battery charging, DC-motor drives, power conversion, etc... [1].

As shown in Fig. 1 AC-DC converters can be classified between topologies working with low switching frequency (line commutated) and other circuits which operate with high switching frequency.

The simplest line-commutated converters use diodes to transform the electrical energy from AC to DC. The use of thyristors allows for the control of energy flow. The main disadvantage of these naturally commutated converters is the generation of harmonics and reactive power [1], [2].

Harmonics have a negative effect in the operation of the electrical system and therefore, an increasing attention is paid to their generation and control [3], [4]. In particular, several standards have introduced important and stringent limits to harmonics that can be injected to the power supply [5], [6], [7].

One basic and typical method to reduce input current harmonics is the use of multipulse connections based on transformers with multiple windings. An additional improvement is the use of passive power filters [3]. In the last decade active filters have been introduced to reduce the harmonics injected to the mains [8], [9], [10].

Another conceptually different way of harmonics reduction is the so called Power Factor Correction (PFC). In these converters, power transistors are included in the power circuit of the rectifier to change actively the waveform of the input current, reducing the distortion [11]. These circuits reduce harmonics and consequently they improve the power factor, which is the origin of their generic name of PFC.

Several PFC topologies like Boost and Vienna rectifiers [12],

[13], [14], [15], are not regenerative and are suited for applications where power is not fed back to the power supply.

However, there are several applications where energy flow can be reversed during the operation. Examples are: locomotives, downhill conveyors, cranes, etc... In all these applications, the line side converter must be able to deliver energy back to the power supply.

This paper is dedicated to this specific type of rectifiers, shown with dashed line in Fig. 1, which operate in four quadrants with a high power factor. These rectifiers, also known as Active Front End (AFE), can be classified as *Voltage Source Rectifiers* (VSR) and *Current Source Rectifiers* (CSR).

The following pages present the most important topologies and control schemes for single and three phase operation. Special attention is dedicated to the application of these converters.
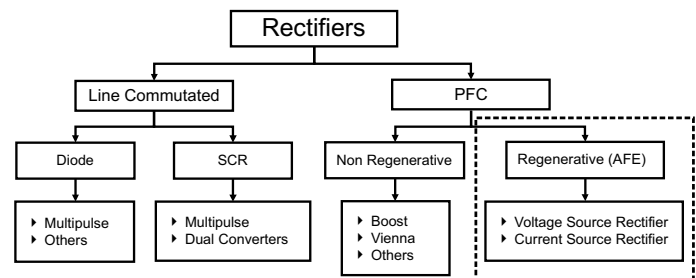

Fig. 1. General classification of rectifiers.

II. PWM VOLTAGE SOURCE RECTIFIERS

A. Single-Phase PWM Voltage Source Rectifiers.

1) Standard for Harmonics in Single-Phase Rectifiers: The relevance of the problems originated by harmonics in line-commutated single-phase rectifiers has motivated some agencies to introduce restrictions to these converters. The IEC 61000-3-2 International Standard establishes limits to all low-power single-phase equipment having an input current with a "special wave shape" and an active input power P<600W. The class D equipment has an input current with a special wave shape contained within the envelope given in Fig. 2-b). This class of equipment must satisfy certain harmonic limits. It is clear that a single-phase line-commutated rectifier shown in Fig. 2-a) is not able to comply with the standard IEC 61000-3-2 Class D as shown in Fig. 3. For traditional rectifiers the standard can be satisfied only by adding huge passive filters, which increases the size, weight and cost of the rectifier. This standard has been the motivation for the development of active methods to improve the quality of the input current and, consequently, the power factor.
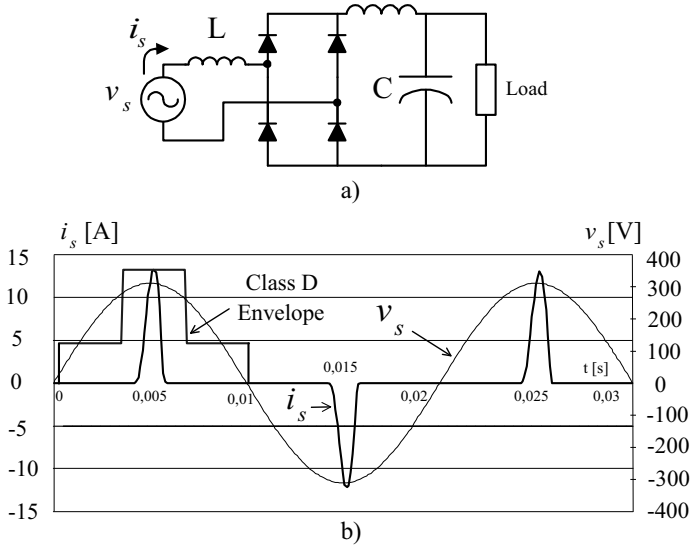
a)

b)

Fig. 2. Single-phase rectifier: a) circuit; b) waveforms of the input voltage and current.
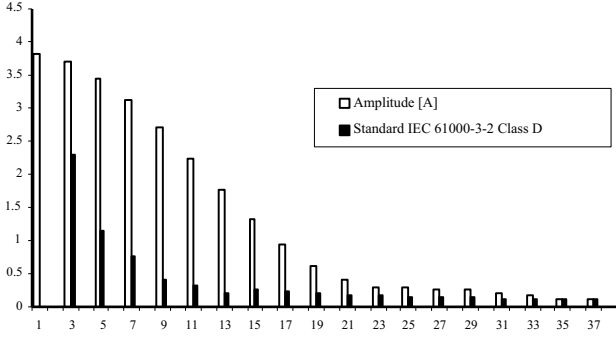

Fig. 3. Harmonics in the input current of the rectifier of Fig. 2-a)

a)

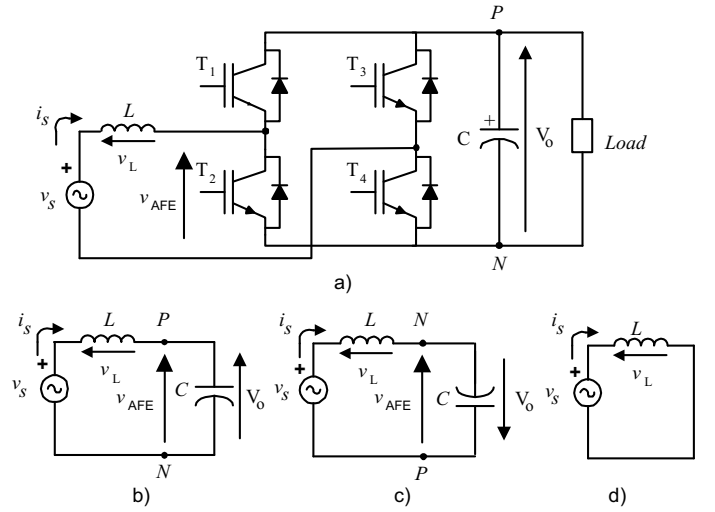b)   c)   d)

Fig. 4. Single-phase PWM rectifier in bridge connection. a) power circuit. Equivalent circuit with b) T_1 and T_4 ON; c) T_2 and T_3 ON ; d) T_1 and T_3 or T_2 and T_4 ON.
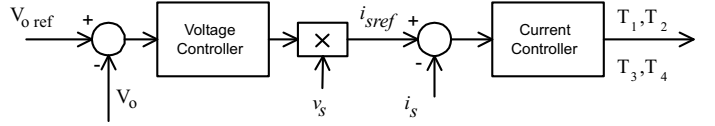

Fig. 5. Control scheme of bridge PWM Rectifier.

2) The Bridge connected PWM Rectifier:

a) Power circuit and working principle: Fig. 4-a) shows the power circuit of the fully controlled single-phase PWM rectifier in bridge connection [16], which uses four transistors with antiparallel diodes to produce a controlled DC voltage V_o. For an appropriated operation of this rectifier, the output voltage must be greater than the input voltage, at any time $(V_o > \widehat{V}_s)$. This rectifier can work with two (bipolar PWM) or three (unipolar PWM) levels as shown in Fig. 4.

The possible combinations are:

  i Switch T_1 and T_4 are in ON state and T_2 and T_3 are in OFF state, $v_{AFE} = V_o$. (Fig. 4-b))
  ii Switch T_1 and T_4 are in OFF state and T_2 and T_3 are in ON state, $v_{AFE} = -V_o$. (Fig. 4-c))
 iii Switch T_1 and T_3 are in ON state and T_2 and T_4 are in OFF state, or T_1 and T_3 are in OFF state and T_2 and T_4 are in ON state, $v_{AFE}= 0$. (Fig. 4-d)).

The inductor voltage can be expressed as:

$$v_L = L\frac{di_s}{dt} = v_s(t) - kV_o \tag{1}$$

where k=1,-1 or 0.
If k=1, then the inductor voltage will be negative, so the input current i_s will decrease its value.

If k=-1, then the inductor voltage will be positive, so the input current i_s will increase its value.
Finally, if k=0 the input current increase or decrease its value depending of v_s. This allows for a complete control of the input current.

b) Control scheme: The classical control scheme is shown in Fig. 5. The control includes a voltage controller, typically a Proportional-Integrative (PI) controller, which controls the amount of power required to maintain the DC-link voltage constant. The voltage controller delivers the amplitude of the input current. For this reason, the voltage controller output is multiplied by a sinusoidal signal with the same phase and frequency than v_s, in order to obtain the input current reference, i_{sref}. The fast current controller controls the input current, so the high input power factor is achieved. This controller can be a hysteresis or a linear controller with a PWM-modulator [17].

Fig. 6 shows the behavior of the output voltage and the input current of the PWM rectifier in response to a step change in the load. It can be observed that the voltage is controlled by increasing the current, which keeps its sinusoidal waveform even during transient states.

As seen in Fig. 6, a ripple at twice of power supply frequency $(2\omega_s)$ is present in the DC-link voltage. If this ripple passes throw the voltage controller it will produce a third harmonic component in i_{sref}. This harmonic can be reduced with a low-pass filter at the voltage measurement reducing the controller bandwidth.

Fig. 7 shows the behavior of voltage and current delivered by the source. The input current is highly sinusoidal and keeps
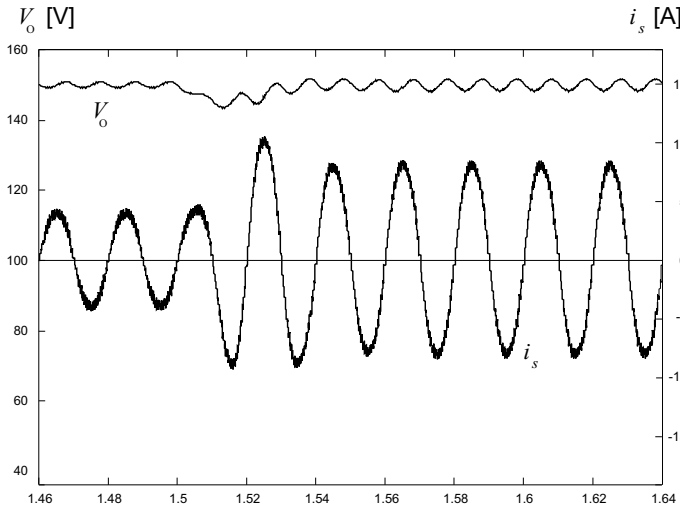
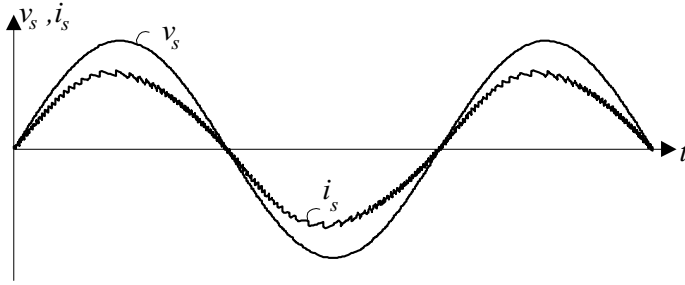Fig. 6. DC-link voltage and input current with 50% load step.

Fig. 7. Waveform of the input current during normal operation.

in phase with the voltage, reaching a very high power factor of PF≈0.99.

Fig. 8 presents the waveforms of voltage and current when the rectifier works in the regeneration mode. Even in this case, the input current is highly sinusoidal.

3) The Voltage Doubler PWM Rectifier:

a) Power circuit and working principle: Fig. 9 shows the power circuit of the voltage doubler PWM rectifier. This topology uses only two power switches T_1 and T_2, which are switched complementary to control the DC-link voltage and the input current, but requires two filter capacitors C_1 and C_2. The voltage on each capacitor (V_{C1}, V_{C2}) must be higher than
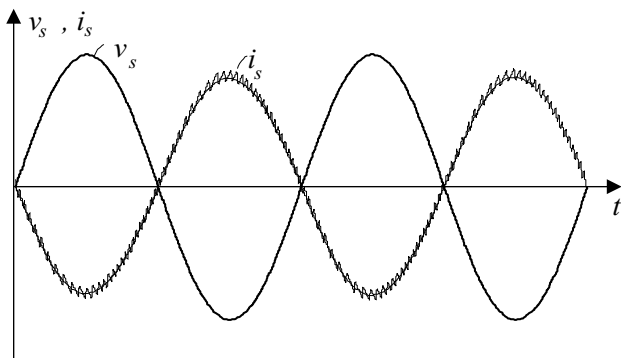

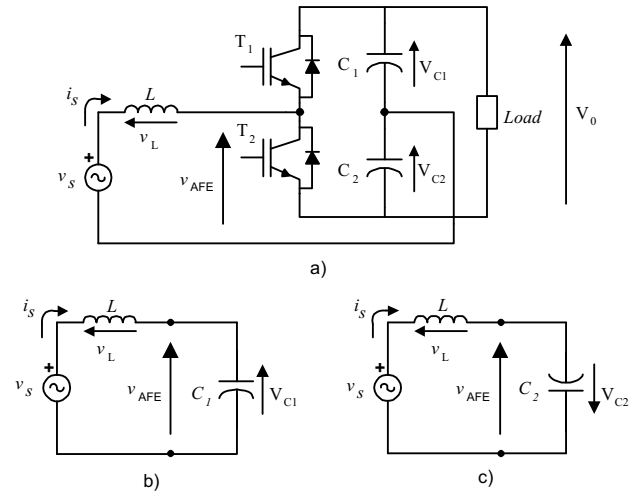Fig. 8. Waveform of the input current during regeneration.

Fig. 9. Single-phase PWM rectifier in voltage doubler connection: a) power circuit; b) equivalent circuit with T_1 ON; c) equivalent circuit with T_2 ON.

the peak value of v_s to ensure the control of the input current. The possible combinations are:

i. Switch T_1 is in ON state $\Rightarrow v_{AFE} = V_{C1}$, so the inductor voltage is:

$$v_L = L\frac{di_s}{dt} = v_s(t) - V_{C1} < 0 \qquad (2)$$

as v_L is negative, the input current will decrease its value.

ii. Switch T_2 is in ON state $\Rightarrow v_{AFE} = -V_{C2}$, so the inductor voltage is:

$$v_L = L\frac{di_s}{dt} = v_s(t) + V_{C2} > 0 \qquad (3)$$

as v_L is positive, the input current will increase its value.

Therefore the waveform of the input current can be controlled by switching appropriately transistors T_1 and T_2 in a similar way as in the bridge connected PWM rectifier.

b) Control scheme: The control scheme for this topology is almost the same than the control for the bridge connection as seen in Fig. 10. The most important difference is the necessity of a controller for voltage balance between both capacitors. A simple P controller is used to achieve this balance [18].
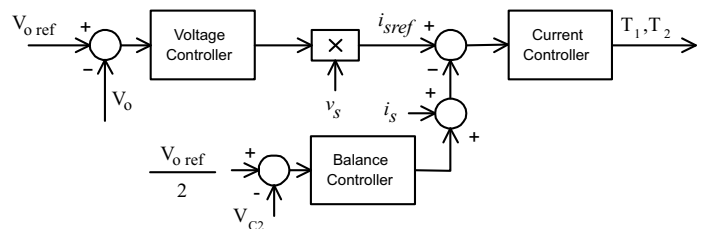

Fig. 10. Control scheme of the voltage doubler PWM Rectifier.

B. Three-Phase Voltage-Source Rectifiers

1) Power circuit and working principle: It is well known that Voltage Source Inverters (VSI), like the one shown in Fig. 11, can work in four quadrants. In two of these quadrants, the VSI works as a rectifier, that means, as a Voltage Source
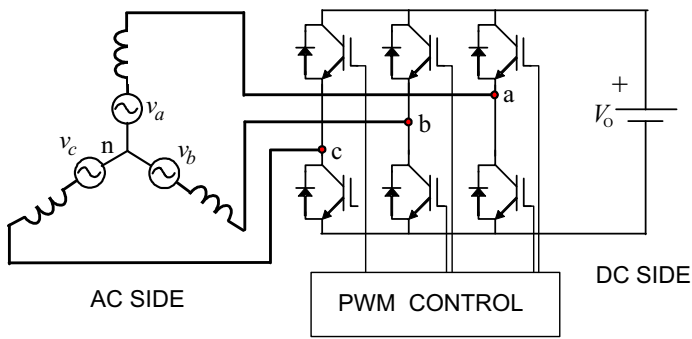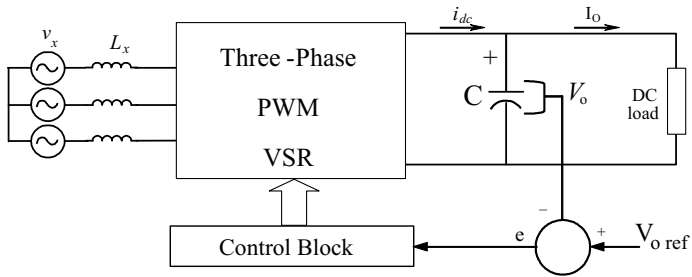
Fig. 11.   Voltage Source PWM Inverter (VSI).

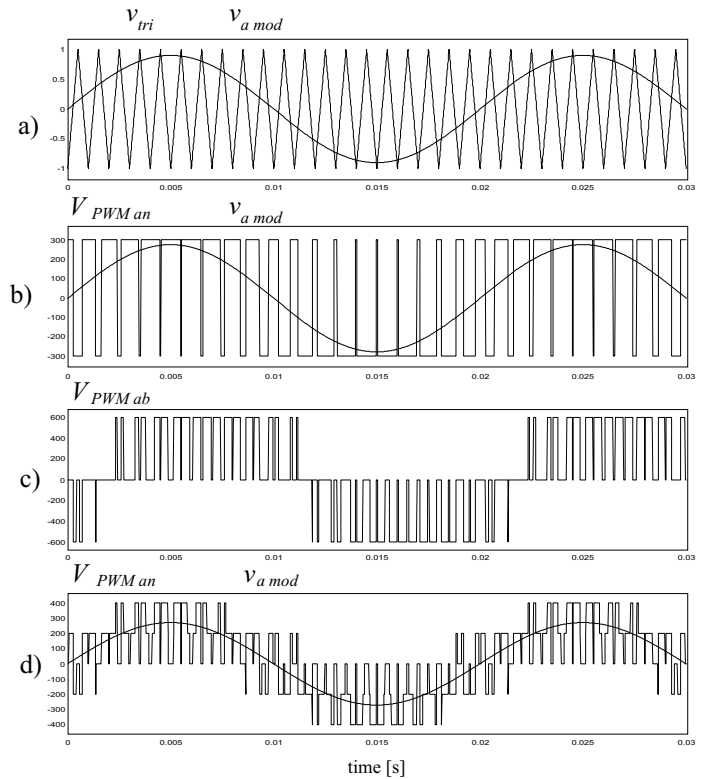Fig. 12.   Operation principle of the VSR.

Fig. 13.   PWM phase voltages. a) triangular carrier and sinusoidal reference, b) PWM phase modulation, c) PWM phase-to-phase voltage, and d) PWM phase-to-neutral voltage.

Rectifier or VSR. However, a stand-alone VSR requires a special DC bus able to keep a voltage V_o without the requirement of a voltage supply. This is accomplished with a dc capacitor C and a feedback control loop.

The basic operation principle of VSR consists on keeping the load DC-link voltage at a desired reference value, using a feedback control loop as shown in Fig. 12 [19]. This reference value $V_{o\ ref}$, has to be high enough to keep the diodes of the converter blocked. Once this condition is satisfied, the DC-link voltage is measured and compared with the reference $V_{o\ ref}$. The error signal generated from this comparison is used to switch ON and OFF the valves of the VSR. In this way, power can come or return to the AC source according with the DC-link voltage value.

When the DC load current I_o is positive (rectifier operation), the capacitor C is being discharged, and the error signal becomes positive. Under this condition, the Control Block takes power from the supply by generating the appropriate PWM signals for the six power transistor of the VSR. In this way, current flows from the AC to the DC side, and the capacitor voltage is recovered. Inversely, when I_o becomes negative (inverter operation), the capacitor C is overcharged, and the error signal asks the control to discharge the capacitor returning power to the AC mains.

The modulator switches the valves ON and OFF, following a pre-established template. Particularly, this template could be a sinusoidal waveform of voltage (voltage source, voltage controlled PWM rectifier) or current (voltage source, current controlled PWM rectifier). For example, for a voltage controlled rectifier, the modulation could be as the one shown in Fig. 13, which has a fundamental called $v_{x\ mod}$ (see Fig. 35), proportional to the amplitude of the template. There are many methods of modulation [22], being the most popular the

so called Sinusoidal Pulse Width Modulation (SPWM), which uses a triangular carrier (v_{tri}) to generate the PWM patron.

To make the rectifier work properly, the PWM pattern must generate a fundamental $v_{x\ mod}$ with the same frequency of the power source v_x. Changing the amplitude of this fundamental, and its phase-shift with respect to the mains, the rectifier can be controlled to operate in the four quadrants: leading power factor rectifier, lagging power factor rectifier, leading power factor inverter, and lagging power factor inverter. Changing the pattern of modulation, modifies the magnitude of $v_{x\ mod}$, and displacing the PWM pattern changes the phase-shift.

The PWM control not only can manage the active power, but reactive power also, allowing the VSR to correct power factor. Besides, the AC current waveforms can be maintained almost sinusoidal, reducing harmonic contamination to the mains supply.

The interaction between $v_{x\ mod}$ and v_x can be seen through a phasor diagram. This interaction permits to understand the four-quadrant capability of this kind of rectifier. In Fig. 14, the following operations are displayed: a) rectifier at unity power factor, b) inverter at unity power factor, c) capacitor (zero power factor), and d) inductor (zero power factor).

Current I_x in Fig. 14 is the *rms* value of the source current i_x. This current flows through the semiconductors in the way shown in Fig. 15. During the positive half cycle, transistor T_N, connected at the negative side of the DC-link is switched ON, and current i_x begins to flow through T_N (i_{Tn}). The current returns to the mains and comes back to the valves,
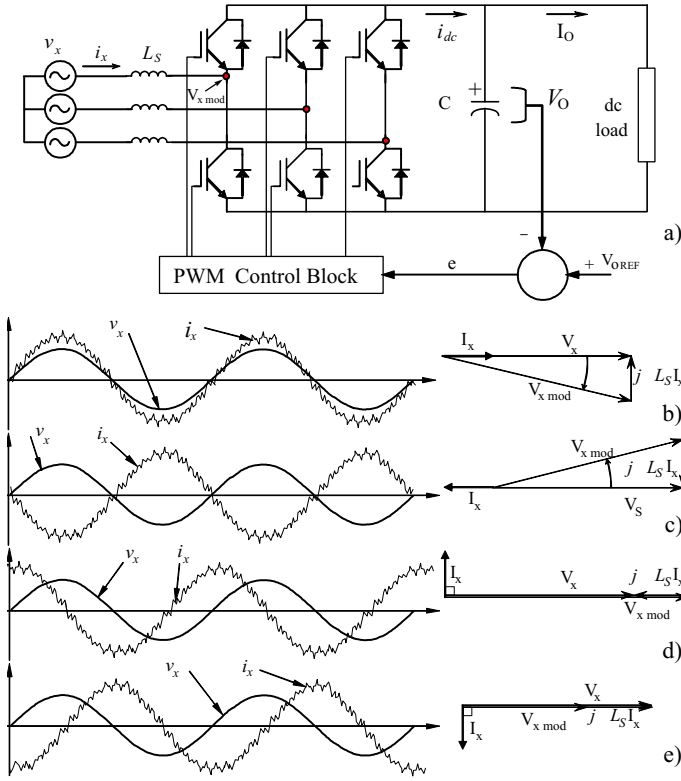
Fig. 14. Four-quadrant operation of the VSR. a) the PWM force commutated rectifier, b) rectifier operation at unity power factor, c) inverter operation at unity power factor, d) capacitor operation at zero power factor, and e) inductor operation at zero power factor.

Fig. 15. Current waveforms through the mains, the valves, and the DC-link.

closing a loop with another phase, and passing through a diode connected at the same negative terminal of the DC-link. The current can also go to the dc load (inversion) and return through another transistor located at the positive terminal of the DC-link. When transistor T_N is switched OFF, the current path is interrupted, and the current begins to flow through diode D_P, connected at the positive terminal of the DC-link. This current, called i_{Dp} in Fig. 15, goes directly to the DC-link, helping in the generation of current i_{dc}, which charges capacitor C and permits the rectifier to produce dc power. Inductances L_s are very important in this process, because they generate an induced voltage which allows for the conduction of diode D_P. Similar operation occurs during the negative half cycle, but with T_P and D_N. Under inverter operation, the current paths are different because the currents flowing through the transistors come mainly from the DC capacitor C. Under rectifier operation, the circuit works like a Boost converter, and under inverter it works as a Buck converter.

2) Control Scheme:

a) Control of the DC-link voltage: The control of the DC-link voltage requires a feedback control loop. As it was already explained in section II-B, the DC voltage V_o is compared with a reference $V_{o\ ref}$, and the error signal "e" obtained from this comparison is used to generate a template waveform. The template should be a sinusoidal waveform with the same frequency of the mains supply. This template is used to produce the PWM pattern, and allows controlling the
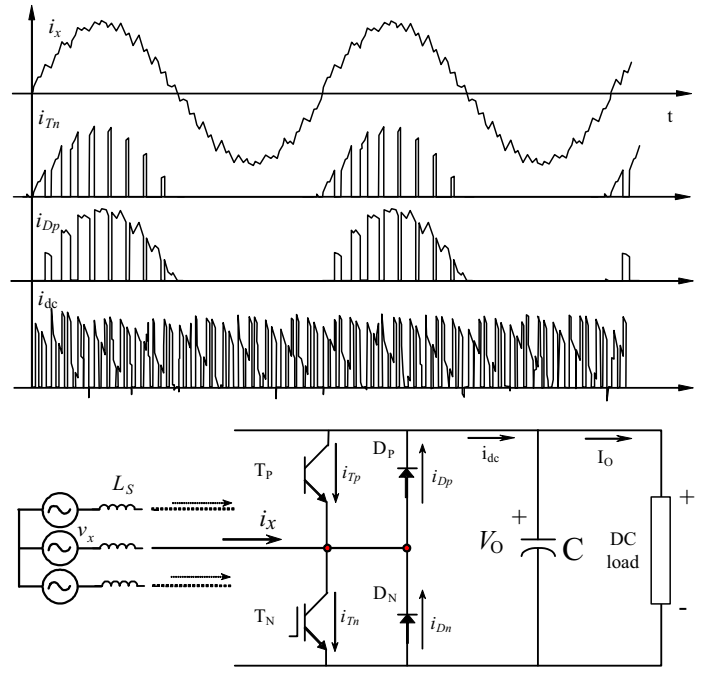
rectifier in two different ways: 1) as a voltage source current controlled PWM rectifier, or 2) as a voltage source voltage controlled PWM rectifier. The first method controls the input current, and the second controls the magnitude and phase of the voltage $v_{x\ mod}$. The current controlled method is simpler and more stable than the voltage-controlled method, and for these reasons it will be explained first.

b) Voltage source current controlled PWM rectifier: This method of control is shown in the rectifier of Fig. 16. The control is achieved by measuring the instantaneous phase currents and forcing them to follow a sinusoidal current reference template, I_{ref}. The amplitude of the current reference template, $\widehat{I}$, is evaluated using the following equation:

$$\widehat{I} = G_c e = G_c(V_{o\ ref} - V_o) \tag{4}$$

Where G_c is shown in Fig. 16, and represents a controller such as PI, P, Fuzzy or other. The sinusoidal waveform of the template is obtained by multiplying $\widehat{I}$ with a sine function, with the same frequency of the mains, and with the desired phase-shift angle, as shown in Fig. 16.

However, one problem arises with the rectifier, because the feedback control loop on the voltage V_o can produce instability [20]. Then, it is necessary to analyze this problem during the design of the rectifier. According to stability criteria, and assuming a PI controller, the following relations are obtained:

$$I_x \leq \frac{CV_o}{3K_pL_s} \tag{5}$$

$$I_x \leq \frac{K_pV_x}{2RK_p + L_sK_i} \tag{6}$$

These two relations are useful for the design of the current controlled VSR. They relate the values of DC-link capacitor, DC-link voltage, *rms* voltage supply, input resistance and inductance, and input power factor, with the *rms* value of the
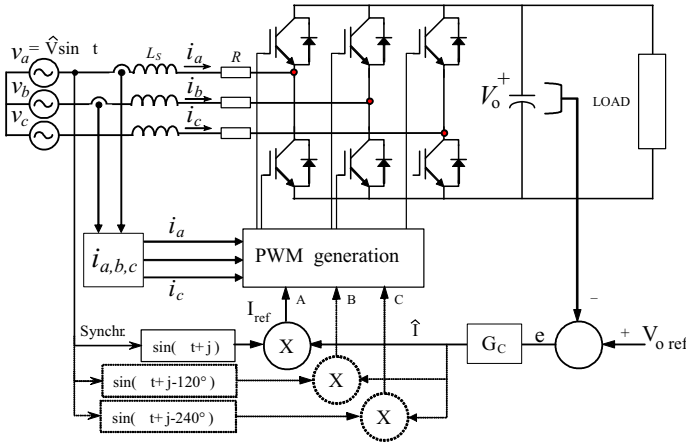
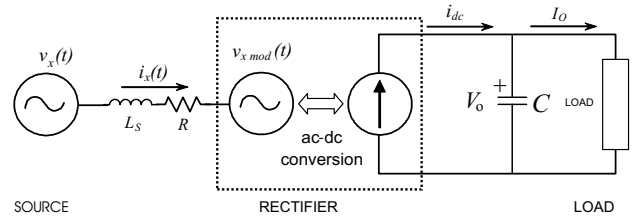Fig. 16. Voltage source current controlled PWM rectifier

Fig. 17. One-phase fundamental diagram of the voltage source rectifier.

Fig. 18. Implementation of the voltage controlled rectifier for unity power factor operation.

input current, I_x. With these relations the proportional and integral gains, K_p and K_i, can be calculated to ensure stability of the rectifier. These relations only establish limitations for rectifier operation, because negative currents always satisfy the inequalities.

With these two stability limits satisfied, the rectifier will keep the DC capacitor voltage at the value of $V_{o\ ref}$ (PI controller), for all load conditions, by moving power from the AC to the DC side. Under inverter operation, the power will move in the opposite direction.

Once the stability problems have been solved, and the sinusoidal current template has been generated, a modulation method will be required to produce the PWM pattern for the power valves. The PWM pattern will switch the power valves to force the input currents I_x, to follow the desired current template I_{ref}. There are many modulation methods in the literature, but three methods for voltage source current controlled rectifiers are the most widely used: *Periodical Sampling* (PS), *Hysteresis Band* (HB), and *Triangular Carrier* (TC).

c) Voltage Source voltage controlled PWM rectifier:
Fig. 17 shows a single-phase diagram from which the control system for a voltage source voltage controlled rectifier is derived [21]. This diagram represents an equivalent circuit of the fundamentals, i.e, pure sinusoidal at the mains side, and pure DC at the DC-link side. The control is achieved by creating a sinusoidal voltage template $v_{x\ mod}$, which is modified in amplitude and angle to interact with the mains voltage v_x. In this way the input currents are controlled without measuring them. Voltage $v_{x\ mod}$ is generated using the differential equations that govern the rectifier.

From Fig. 17 the following differential equation can be derived:

$$v_x(t) = L_s \frac{di_x}{dt} + Ri_x + v_{x\ mod}(t) \qquad (7)$$

Assuming that $v_x(t) = \widehat{V} \sin(\omega t + \varphi)$, then the solution for $i_x(t)$, to get a voltage $v_{x\ mod}$ able to make the rectifier work at constant power factor should be of the form:

$$i_x(t) = \widehat{I}(t) \sin(\omega t + \varphi) \qquad (8)$$
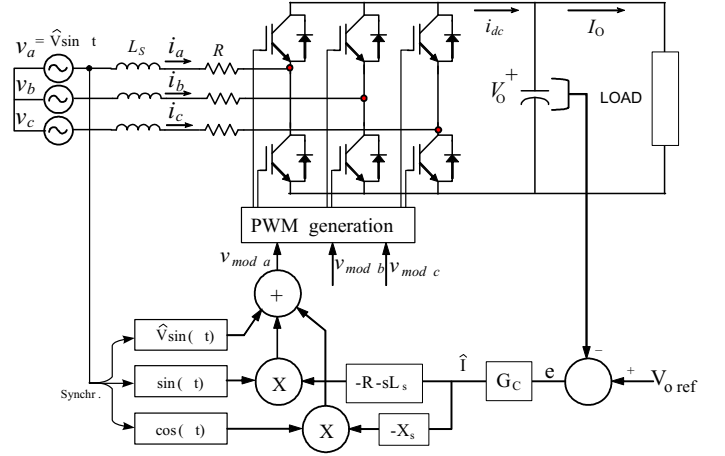
Equations (7), (8), and $v_x(t)$ allow to get a function of time able to modify $v_{x\ mod}$ in amplitude and phase, which will make the rectifier work at fixed power factor. Combining these equations with $v_x(t)$, yields:

$$v_{x\ mod} = \left[X_s \widehat{I} \sin\varphi + \left(\widehat{V} - R\widehat{I} - L_s \frac{d\widehat{I}}{dt} \right) \cos\varphi \right] \sin\omega t$$
$$- \left[X_s \widehat{I} \cos\varphi + \left(R\widehat{I} + L_s \frac{d\widehat{I}}{dt} - \widehat{V} \right) \sin\varphi \right] \cos\omega t \qquad (9)$$

This equation can also be written for unity power factor operation. In such a case $\cos\varphi = 1$, and $\sin\varphi = 0$:

$$v_{x\ mod} = \left(\widehat{V} - R\widehat{I} - L_s \frac{d\widehat{I}}{dt} \right) \sin\omega t - X_s \widehat{I} \cos\omega t \qquad (10)$$

The implementation of the voltage controlled rectifier for unity power factor operation is shown in Fig. 18. It can be observed that there is no need to sense the input currents. However, to ensure stability limits as good as the limits of the current controlled rectifier of Fig. 16, blocks $-R - sL_s$ and $-X_s$ in Fig. 18, have to emulate and reproduce exactly the real values of R, X_s and L_s of the power circuit. However, these parameters do not remain constant, and this fact affects the stability of this system, making it less stable than the system shown in Fig. 16.

d) Space-Vector Control: Another point of view is to control the three-phase VSR in *d-q* vector space. The input
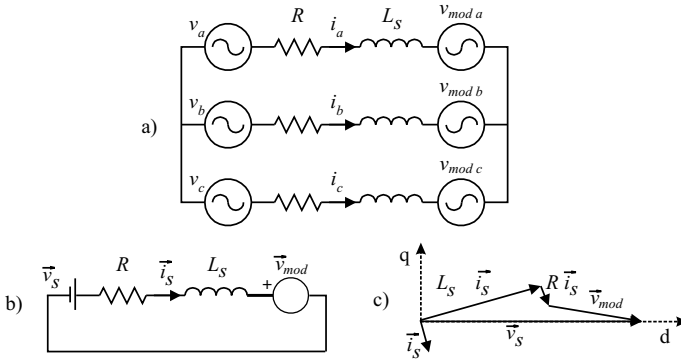
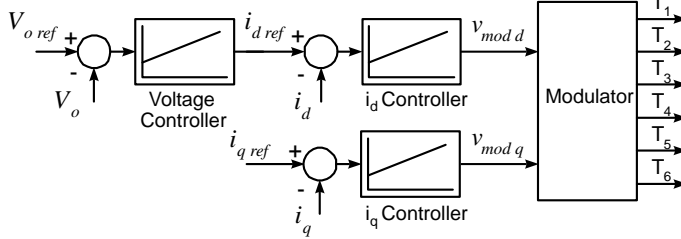Fig. 19. Power circuit a) before transformation; b) after transformation. c)d-q space vector quantities.

Fig. 20. Space-Vector control scheme.

currents i_a, i_b and i_c can be represented by a unique complex vector $\vec{i}_s = i_d + j\,i_q$, defined by:

$$\begin{bmatrix} i_d \\ i_q \end{bmatrix} = \frac{2}{3} \begin{bmatrix} \cos\theta & \sin\theta \\ -\sin\theta & \cos\theta \end{bmatrix} \begin{bmatrix} 1 & -\frac{1}{2} & -\frac{1}{2} \\ 0 & \frac{\sqrt{3}}{2} & -\frac{\sqrt{3}}{2} \end{bmatrix} \begin{bmatrix} i_a \\ i_b \\ i_c \end{bmatrix} \quad (11)$$

where $\theta = \omega_s t$.

This transformation can be applied to

$$v_{mod} = \begin{bmatrix} v_{mod\ a} \\ v_{mod\ b} \\ v_{mod\ c} \end{bmatrix}$$

fundamental component of the VSR PWM voltages defined in II-B.1, and to $v_s = [v_a\ v_b\ v_c]'$, where can be demonstrated that the voltage vector obtained is $\vec{v}_s = v_d$, and that the angle between $\vec{i}_s$ and $\vec{v}_s$ correspond to the shift between the input current and the input voltage of each phase.

The power circuit obtained with this transformation and the control scheme are presented in Figs. 19 and 20.

The DC-link voltage V_o is controlled by a PI regulator, which provides the value of $i_{d\ ref}$, while $i_{q\ ref}$ is fixed to zero in order to obtain power factor 1. These references are compared with the input currents which are in d-q coordinates according to (11). Two controllers, typically PI, give the values $v_{mod\ d}$ and $v_{mod\ q}$ to be generated by the VSR.

The gate drive pulses for the transistors $T_1 \ldots T_6$, can be obtained in two ways: transforming $v_{mod\ d}$ and $v_{mod\ q}$ to α-β vector space according to:

$$\begin{bmatrix} v_{mod\ \alpha} \\ v_{mod\ \beta} \end{bmatrix} = \begin{bmatrix} \cos\theta & -\sin\theta \\ \sin\theta & \cos\theta \end{bmatrix} \begin{bmatrix} v_{mod\ d} \\ v_{mod\ q} \end{bmatrix} \quad (12)$$

and a *Space Vector Modulation* (SVM) scheme, or applying the complete inverse transformation:

$$\begin{bmatrix} v_{mod\ a} \\ v_{mod\ b} \\ v_{mod\ c} \end{bmatrix} = \begin{bmatrix} 1 & 0 \\ -\frac{1}{2} & \frac{\sqrt{3}}{2} \\ \frac{1}{2} & -\frac{\sqrt{3}}{2} \end{bmatrix} \begin{bmatrix} \cos\theta & -\sin\theta \\ \sin\theta & \cos\theta \end{bmatrix} \begin{bmatrix} v_{mod\ d} \\ v_{mod\ q} \end{bmatrix} \quad (13)$$

and using a *SPWM* as shown in Fig. 13.

III. PWM CURRENT SOURCE RECTIFIERS

Current source rectifiers (CSRs) are the dual of voltage source rectifiers (VSRs). In fact, they can produce identical normalized electrical variables for which equivalent gating patterns have been found. This task is performed by the modulating techniques that must ensure that all the special requirements of the topology are met. A general power topology and the control strategy and modulating technique blocks are depicted in Fig. 21.

A. Power circuit and working principle

The main objective of these static power converters is to produce a controllable DC current waveform from the AC power supply (see Fig. 21). Due to the fact that the resulting AC line currents $i_r = [i_{ra}\ i_{rb}\ i_{rc}]'$ feature high *di/dt* and the unavoidable inductive nature of the AC mains, a capacitive filter should be placed in between. Thus, nearly sinusoidal supply currents $i_s = [i_{sa}\ i_{sb}\ i_{sc}]'$ are generated that justifies the use of such topologies in medium-voltage adjustable speed drives (ASDs), where high-quality waveforms are required. Due to the fact that the CSR can be modelled as a controllable DC current source, the natural load is a current source inverter (CSI) as in ASDs [23]. Additionally, the positive nature of the DC current i_{dc} and the bipolarity of the DC voltage V_o constrains the type of power valves to unidirectional switches with reverse voltage block capability as in GTOs and the recently introduced IGCT [24].

In order to properly gate the power switches of a three-phase CSR topology, two main constraints must always be met: (a) the AC side is mainly capacitive, thus, it must not be short-circuited; this implies that, at most one top switch (S_1, S_3, or S_5) and one bottom switch (S_4, S_6, or S_2) should be closed at any time; and (b) the DC bus is of the current-source type and thus it cannot be opened; therefore, there must be at least one top switch and one bottom switch closed at all times, Fig. 21. Both constraints can be summarized by stating that at any time, only one top switch and one bottom switch must be closed [25]. The constraints are reduced to nine valid states in three-phase CSRs, where states 7, 8, and 9 (Table I) produce zero AC line currents, i_r. In this case, the DC-link current freewheels through either the switches S_1 and S_4, S_3 and S_6, or S_5 and S_2.

There are several modulating techniques that deal with the special requirements of the gating patterns of CSRs and can be implemented online. Among them are: (a) the carrier-based; (b) the selective harmonic elimination; (c) the selective harmonic equalization, and (d) the space-vector technique.

TABLE I
VALID SWITCH STATES FOR A THREE-PHASE CSR.

State	State	i_{ra}	i_{rb}	i_{rc}
S_1, S_2 ON; S_3, S_4, S_5, S_6 OFF	1	i_{DC}	0	$-i_{DC}$
S_2, S_3 ON; S_4, S_5, S_6, S_1 OFF	2	0	i_{DC}	$-i_{DC}$
S_3, S_4 ON; S_5, S_6, S_1, S_2 OFF	3	$-i_{DC}$	i_{DC}	0
S_4, S_5 ON; S_6, S_1, S_2, S_3 OFF	4	$-i_{DC}$	0	i_{DC}
S_5, S_6 ON; S_1, S_2, S_3, S_4 OFF	5	0	$-i_{DC}$	i_{DC}
S_6, S_1 ON; S_2, S_3, S_4, S_5 OFF	6	i_{DC}	$-i_{DC}$	0
S_1, S_4 ON; S_2, S_3, S_5, S_6 OFF	7	0	0	0
S_3, S_6 ON; S_1, S_2, S_4, S_5 OFF	8	0	0	0
S_5, S_2 ON; S_6, S_1, S_3, S_4 OFF	9	0	0	0
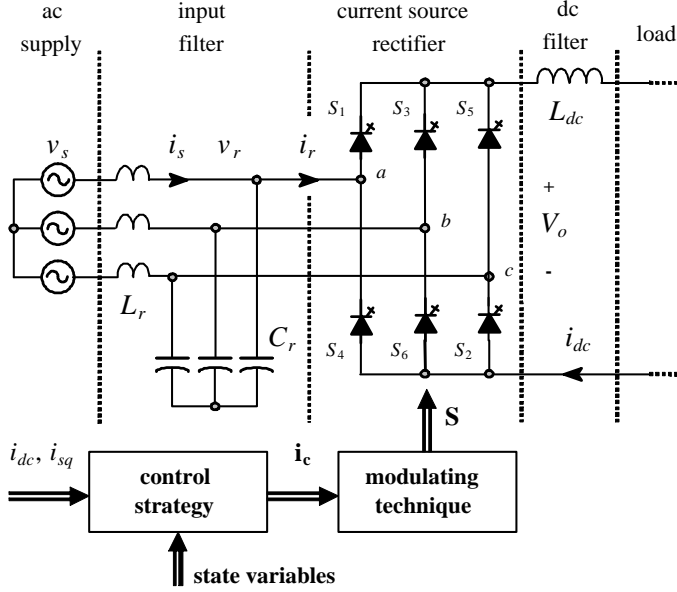
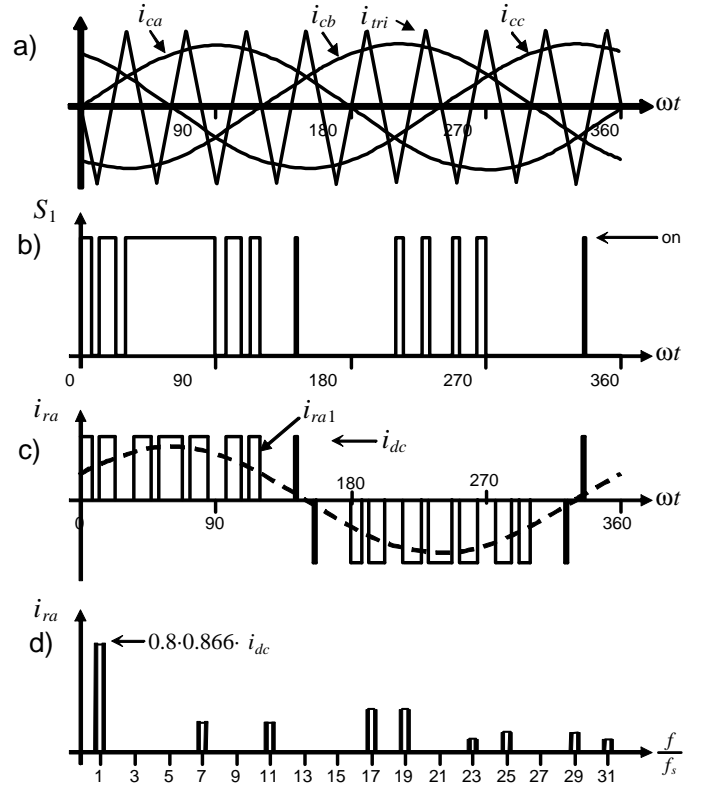Fig. 21.   Three-phase CSR topology, modulation, and control.

Fig. 22.   The three-phase CSR ideal waveforms for the SPWM: a) carrier and modulating signals; b) switch S_1 state; c) AC current; d) AC current spectrum.

B. Control Scheme

1) Modulating Techniques: The modulating techniques use a set of AC normalized current references $i_c = [i_{ca}\ i_{cb}\ i_{cc}]'$ that should be sinusoidal in order to obtain nearly sinusoidal supply AC currents (i_s), as shown in Fig. 21. To simplify the analysis, a constant DC-link current source is considered ($i_{DC} = I_{DC}$).

a) Carrier-based Techniques.: It has been shown that carrier-based PWM techniques that were initially developed for three-phase voltage source inverters (VSIs) can be extended to three-phase CSRs. In fact, the circuit detailed in [25] obtains the gating pattern for a CSR from the gating pattern developed for a VSI. As a result, the normalized line current is identical to the normalized line voltage in a VSI for similar carrier and modulating signals. Examples of such modulating signals are the standard sinusoidal, sinusoidal with zero sequence injection, trapezoidal, and deadband waveforms. Fig. 22 shows the relevant waveforms if a triangular carrier i_{tri} and sinusoidal modulating signals i_c are used in combination with the gating pattern generator introduced in [25]. It can be observed that the line current waveform (Fig. 22-c) is

identical to the obtained in three-phase VSIs, where a SPWM technique is used. This brings up the duality issue between both topologies when similar modulation approaches are used. Therefore, for odd multiple of 3 values of the normalized carrier frequency m_f, the harmonics in the AC current appear at normalized frequencies f_h centered around m_f and its multiples, specifically, at

$$h = l \cdot m_f \pm k \qquad l = 1, 2, \dots \qquad (14)$$

where $l = 1, 3, 5, \dots$ for $k = 2, 4, 6, \dots$ and $l = 2, 4, \dots$ for $k = 1, 5, 7, \dots$ such that h is not a multiple of 3. For nearly sinusoidal AC voltages v_r, the harmonics in the DC-link voltage , V_o, are at normalized frequencies given by

$$h = l \cdot m_f \pm k \pm 1 \qquad l = 1, 2, \dots \qquad (15)$$

where $l = 0, 2, 4, \dots$ for $k = 1, 5, 7, \dots$ and $l = 1, 3, 5, \dots$ for $k = 2, 4, 6, \dots$ such that $h = lm_f \pm k$ is positive and not a multiple of 3. This analysis shows that for low switching frequencies very low unwanted harmonics will appear. This is a very undesired effect as in CSR there is a second order input filter and resonances could be obtained. This is why selective harmonic elimination is the preferred alternative as it allows to specify the resulting spectra.

b) Selective Harmonic Elimination (SHE): This technique deals directly with the gating patterns of the CSR. It defines the gating signals in order to eliminate some predefined harmonics and control the fundamental amplitud of input

current i_r. Under balanced conditions, the chopping angles are calculated to eliminate only the harmonics at frequencies $h = 5, 7, 11, 13, \ldots$ In [26] is proposed a direct method to obtain the angles to eliminate a given number of harmonics. However, just an even number of harmonics can be eliminated. On the other hand, [27] proposes to use single phase CSRs to form three-phase structures. This alternative alleviates the resulting non-linear equations to be solved; however, the number of power switches increases up to twice as compared to the standard six-switches configuration. Also [28] proposes a method to eliminate an arbitrary number of harmonics, while controlling the fundamental AC current component, by using the results obtained in VSIs [29]. Specifically, the general expressions to eliminate $N - 1$ ($N - 1 = 2, 4, 6, \ldots$, even) harmonics are given by the following equations,

$$-\sum_{k=1}^{N}(-1)^k \cos(n\alpha_k) = \frac{2 + m\pi}{4}$$

$$-\sum_{k=1}^{N}(-1)^k \cos(n\alpha_k) = \frac{1}{2} \quad for \quad n = 5, 7, \ldots 3N - 2$$

$$(16)$$

where $\alpha_1, \alpha_2, \ldots, \alpha_N$ should satisfy $\alpha_1 < \alpha_2 < \cdots < \alpha_N < \pi/2$. Fig. 23-a shows the distribution of α_1, α_2, and α_3 to eliminate the 5th and 7th and Fig. 24 the values as a function of the desired fundamental AC current component. Similarly, the general expressions to eliminate $N - 1$ ($N - 1 = 3, 5, 7, \ldots$, odd) harmonics are,

$$-\sum_{k=1}^{N}(-1)^k \cos(n\alpha_k) = \frac{2 - m\pi}{4}$$

$$-\sum_{k=1}^{N}(-1)^k \cos(n\alpha_k) = \frac{1}{2} \quad for \quad n = 5, 7, \ldots 3N - 1$$

$$(17)$$

where $\alpha_1, \alpha_2, \ldots, \alpha_N$ should satisfy $\alpha_1 < \alpha_2 < \cdots < \alpha_N < \pi/3$.

Fig. 23 shows that the line current does not contain the 5th and the 7th harmonics as expected.

The series/parallel connection of CSRs is used to improve the quality of the waveforms by creating n-pulse converters [23],[30]. In fact, a delta-wye transformer naturally eliminates the 5th and 7th harmonics and, therefore, the first unwanted harmonics are the 12th at the DC side and the 11th and the 13th at the AC side. The series/parallel connection increase the degrees of freedom of the system, so modified SHE algorithms like selective harmonic equalization presented in [31], can be used.

c) Space vector modulation (SVM): The objective is to generate PWM AC line currents i_r that are on average equal to the given references i_c. This is done digitally in each sampling period by properly selecting the switch states from the valid ones of the CSR (Table I) and the proper calculation of the period of times they are used. The selection and time calculations are based upon the space-vector (SV) transformation [32]. The vector of line-modulating signals i_c can be represented by the complex vector $\mathbf{I_c} = [i_{c\alpha} \ i_{c\beta}]'$ by
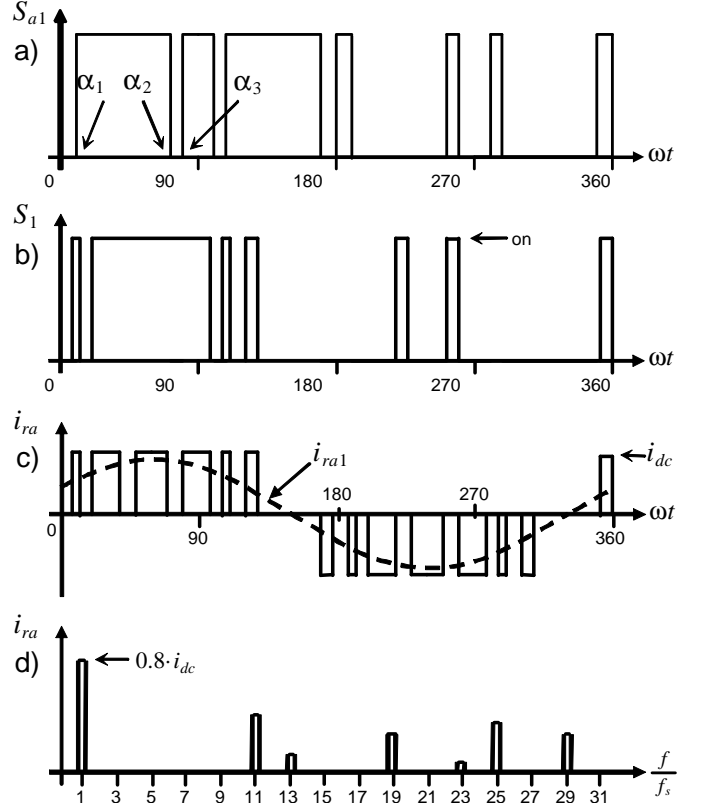

Fig. 23. Waveforms for the SHE technique in CSRs for 5th and 7th harmonic elimination: a) VSI gating pattern; b) CSR gating pattern; c) line current i_{ra}; d) spectrum of (c).
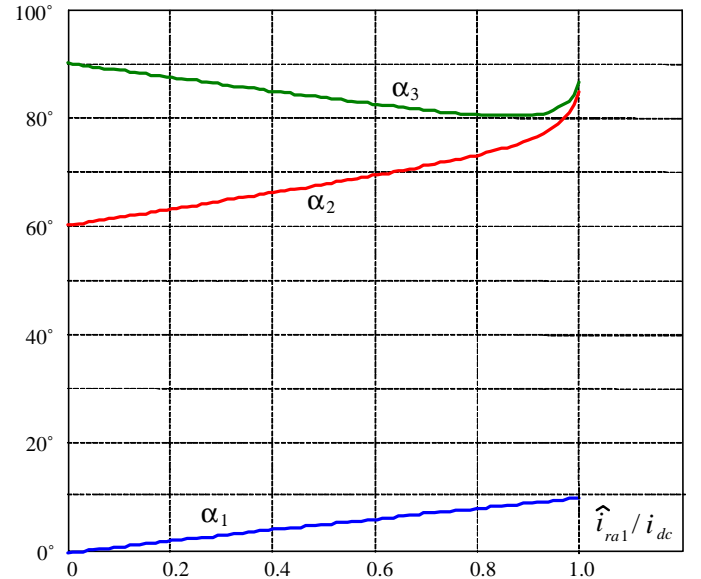

Fig. 24. Chopping angles for 5th and 7th harmonic elimination and fundamental current control in three-phase CSRs.
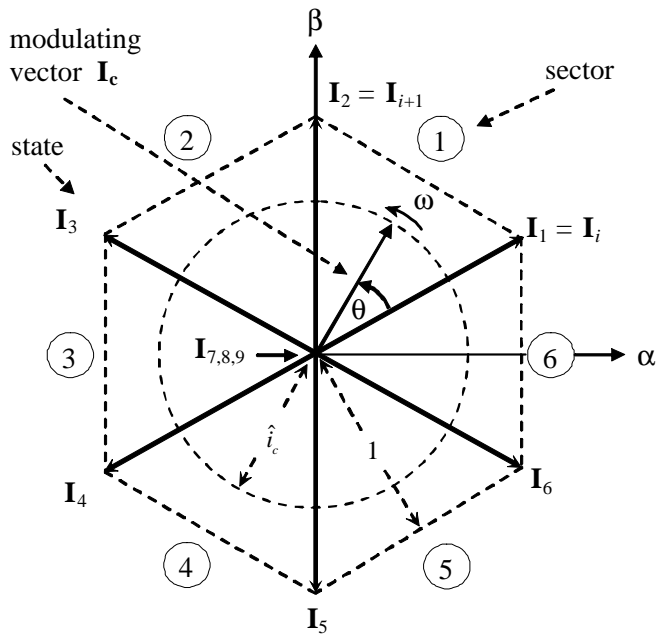
Fig. 25. The space-vector representation in CSIs.

Fig. 26. Ideal waveforms for SV modulation: a) modulating signals; b) switch S_1 state; c) AC current; d) AC current spectrum.

means of,

$$i_{c\alpha} = \frac{2}{3} \left[i_{ca} - 0.5(i_{cb} + i_{cc}) \right] \tag{18}$$

$$i_{c\beta} = \frac{1}{\sqrt{3}} (i_{cb} - i_{cc}) \tag{19}$$

Similarly, the SV transformation is applied to the nine states of the CSR normalized with respect to i_{DC}, which generates nine space vectors ($\mathbf{I_i}$, $i = 1, 2, \ldots, 9$ in Fig. 25). As expected, $\mathbf{I_1}$ to $\mathbf{I_6}$ are nonnull line current vectors and $\mathbf{I_7}$, $\mathbf{I_8}$, and $\mathbf{I_9}$ are null line current vectors.

If the modulating signal vector $\mathbf{I_c}$ is between the arbitrary vectors $\mathbf{I_i}$ and $\mathbf{I_{i+1}}$, then $\mathbf{I_i}$ and $\mathbf{I_{i+1}}$ combined with one zero SV ($\mathbf{I_z} = \mathbf{I_7}$ or $\mathbf{I_8}$ or $\mathbf{I_9}$) should be used to generate $\mathbf{I_c}$. To ensure that the generated current in one sampling period T_s (made up of the currents provided by the vectors $\mathbf{I_i}$, $\mathbf{I_{i+1}}$, and $\mathbf{I_z}$ used during times T_i, T_{i+1}, and T_z) is on average equal to the vector $\mathbf{I_c}$, the following expressions should hold,

$$T_i = T_s \widehat{i_c} \sin\left(\frac{\pi}{3} - \theta\right) \tag{20}$$

$$T_{i+1} = T_s \widehat{i_c} \sin(\theta) \tag{21}$$

$$T_z = T_s - T_i - T_{i+1} \tag{22}$$

where $0 \leq \widehat{i_c} \leq 1$ is the length of the vector $\mathbf{I_c}$. Although, the SVM technique selects the vectors to be used and their respective on-times, the sequence in which they are used, the selection of the zero space vector, and the normalized sampled frequency remain undetermined. The sequence establishes the symmetry of the resulting gating pulses and thus the distribution of the current throughout the power switches. More importantly, the normalized sampling frequency f_{sn} should be an integer multiple of 6 to minimize uncharacteristic harmonics by using evenly the active states of the converter, an important issue at low switc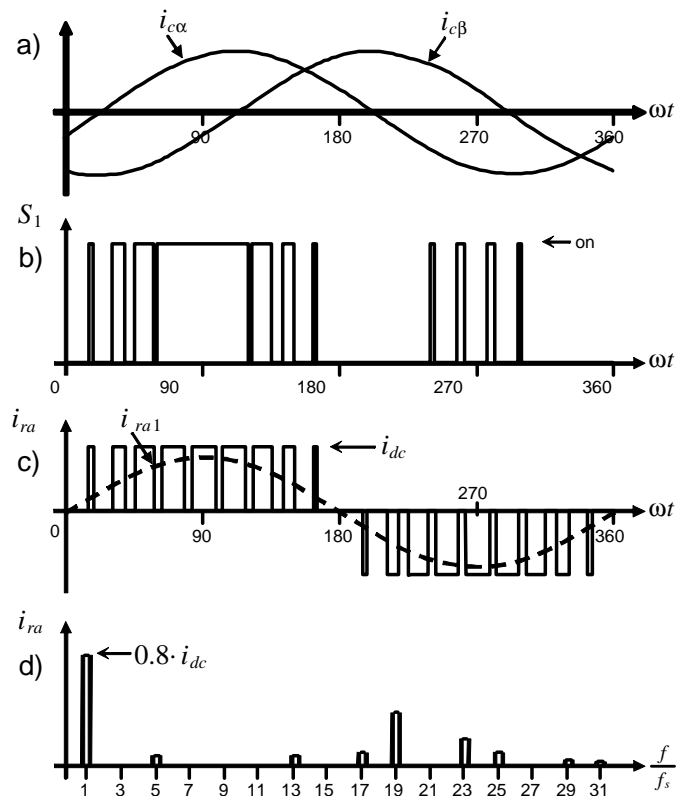hing frequencies. Fig. 26 shows the relevant waveforms of a CSR SVM. It can be seen that the first set of relevant unwanted harmonics in the AC line currents are at f_s.

2) Closed and/or open Loop Operation: The main objective of the CSR is to generate a controllable DC-link current. However, the modulating techniques provide three modulating signals that add up to zero; therefore, there are two degrees of freedom. This rises the issue of being possible to control independently two electrical quantities. Several papers have proposed different control strategies; for instance, synchronous compensation [33], [34], power factor correction [35], [36], active filtering [37], [38], and more importantly, as part of an ASD [23], [39]. All of which control the DC link current (which could also be the active AC current component) and the second is the reactive AC current component. If the control system is synchronized with the AC mains and the setting of the desired reactive AC current component is adjusted to a given: (a) DC value, synchronous compensation is obtained, (b) AC waveform, active filtering is obtained, (c) DC value equal to zero, unity displacement power factor is obtained.

IV. APPLICATIONS OF REGENERATIVE PWM RECTIFIERS

A. Single-phase PWM Voltage Source Rectifiers

1) The PWM Rectifier in Bridge Connection :

a) Single-phase UPS: The distortion of the input current in the line commutated rectifiers with capacitive filtering is particularly critical in uninterruptible power supplies (UPS)
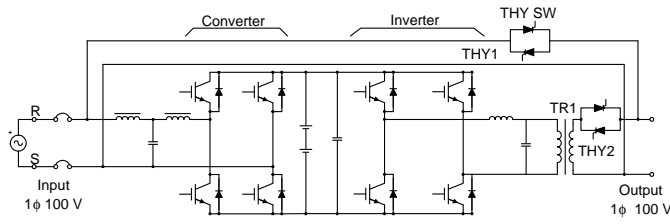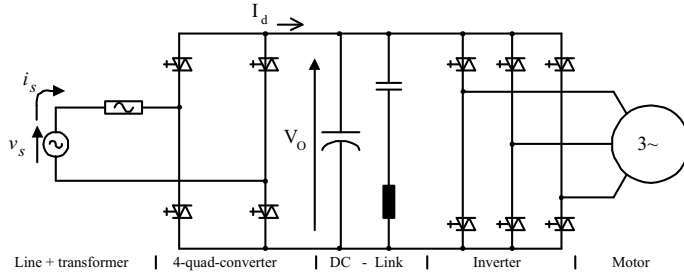
Fig. 27. Single-phase UPS with PWM rectifier.

Fig. 28. Typical power circuit of an AC drive for locomotive.

fed from motor-generator sets. In effect, due to the higher value of the generator impedance, the current distortion can originate an unacceptable distortion on the AC voltage, which affects the behavior of the whole system. For this reason, in this application, it is very attractive to use rectifiers with low distortion in the input current.

Fig. 27 shows the power circuit of a single-phase UPS, which has a PWM rectifier in bridge connection at the input side. This rectifier generates a sinusoidal input current and controls the charge of the battery [43], [44].

b) AC drive for locomotive: One of the most typical and widely accepted areas of application of high power factor single-phase rectifiers is in locomotive drives [40]. In effect, an essential prerequisite for proper operation of voltage source three-phase inverter drives in modern locomotives is the use of four quadrant line-side converters, which ensures motoring and braking of the drive, with reduced harmonics in the input current. Fig. 28 shows a simplified power circuit of a typical drive for a locomotive connected to a single-phase power supply [41], which includes a high power factor rectifier at the input.

Fig. 29 shows the main circuit diagram of the 300 series Shinkansen train [42]. In this application, AC power from the overhead catenary is transmitted through a transformer to single-phase PWM rectifiers, which provide the DC voltage for the inverters. The rectifiers are capable of controlling the input AC current in an approximate sine wave form and in phase with the voltage, achieving power factor close to unity on powering and on regenerative braking. Regenerative braking produces energy savings and an important operational flexibility.

2) The Voltage Doubler PWM Rectifier:

a) Low-cost induction motor drive: The development of low-cost compact motor drive systems is a very relevant topic, particularly in the low-power range. Fig. 30 shows a low cost converter for low power induction motor drives. In this
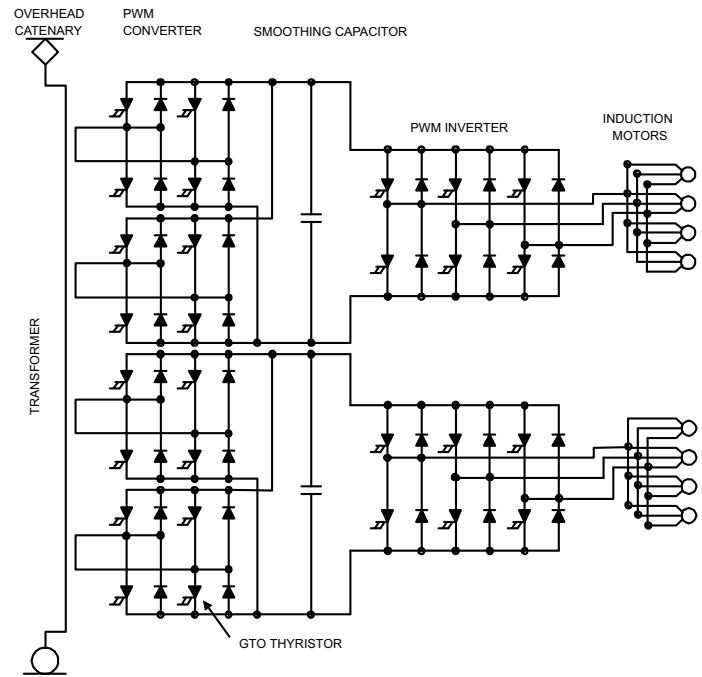

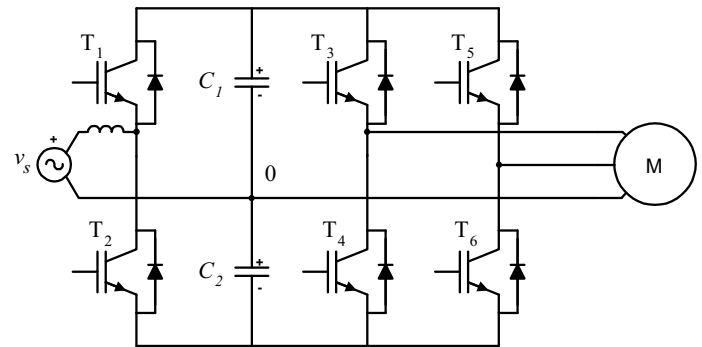Fig. 29. Main circuit diagram of 300 series Shinkansen locomotives.

Fig. 30. Low-cost induction motor drive.

configuration a three-phase induction motor is fed through the converter from a single-phase power supply. Transistors T_1, T_2 and capacitors C_1, C_2 constitute the voltage-doubler single-phase rectifier, which controls the DC-link voltage and generates sinusoidal input current, working with close-to-unity power factor [44]. On the other hand, transistors T_3, T_4, T_5 and T_6 and capacitors C_1 and C_2 constitute the power circuit of an asymmetric inverter that supplies the motor. An important characteristic of the power circuit shown in Fig. 30 is the capability to regenerate power to the single-phase mains.

b) UPS: Another common application for doubler-voltage rectifier is in low cost UPS system as described in [45]. The number of power switches can be decreased from eight to four, as shown in Fig. 31.

B. Three-phase PWM Voltage Source Rectifiers

One of the most important applications of VSR is in machine drives. Fig. 32 shows a typical frequency converter with a force-commutated rectifier-inverter link. The rectifier side controls the input current and the DC-link, and the inverter
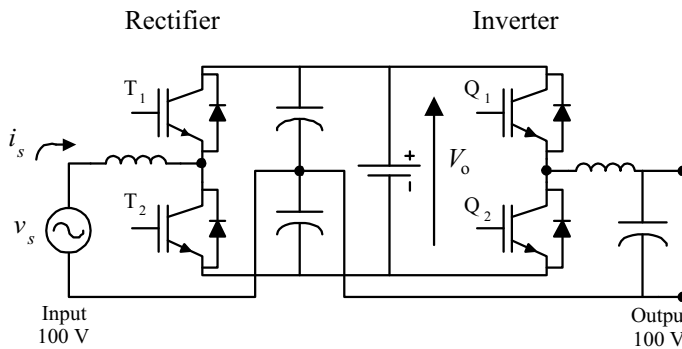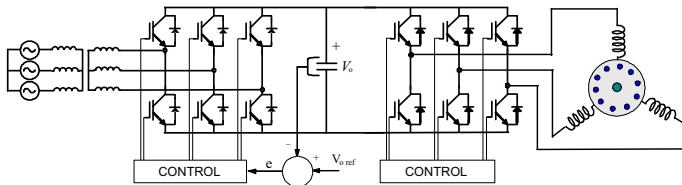
Fig. 31.   UPS with doubler-voltage rectifier.

Fig. 32.   Frequency converter with force commutated rectifier.

Fig. 34.   Variable-speed constant-frequency wind generator.

side controls the machine. The machine can be a synchronous, brushless DC, or induction machine. The reversal of speed and reversal of power are possible with this topology. At the rectifier side, the power factor can be controlled, and even with an inductive load such as an induction machine, the source can "see" the load as capacitive or resistive. The inverter will become a rectifier during regenerative braking, which is possible making slip negative in an induction machine, or making torque angle negative in synchronous and brushless DC machines.

A variation of the drive of Fig. 32 is found in electric traction applications. Battery powered vehicles use the inverter as rectifier during regenerative braking, and sometimes the inverter is also used as battery charger. In this case, the rectifier can be fed by a single-phase or by a three-phase system. Fig. 33 shows a battery powered electric bus system. This system uses the power inverter of the traction motor as rectifier for two purposes: regenerative braking, and battery charger fed by a three-phase power source.

Another application of VSR is in power generation. Power generation at 50 or 60 Hz normally requires constant speed synchronous machines. Besides, induction machines are not currently used in power plants because of magnetization
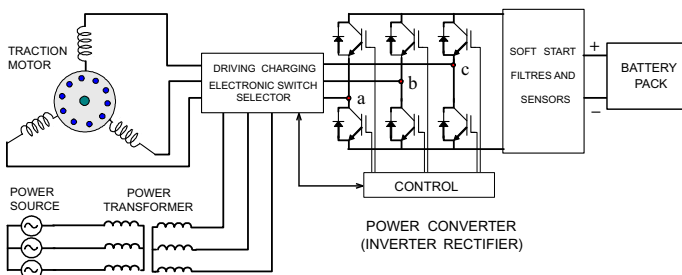

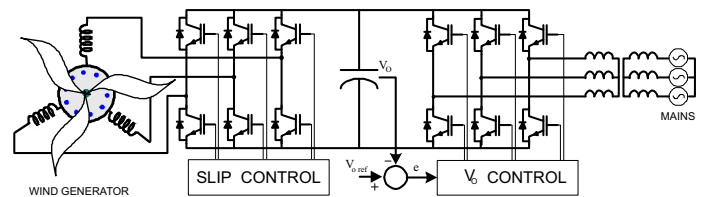Fig. 33.   Electric bus system with regenerative braking and battery charger.

problems. Using frequency-link force-commutated converters, variable-speed constant-frequency generation becomes possible, even with induction generators. The power plant of Fig. 34 shows a wind generator implemented with an induction machine, and a rectifier-inverter frequency link connected to the utility. The DC-link voltage is kept constant with the converter located at the mains side. The converter connected at the machine side controls the slip of the generator and adjusts it according with the speed of wind or power requirements. The utility is not affected by the power factor of the generator, because the two converters keep the $\cos \varphi$ of the machine independent of the mains supply. The last one can even be adjusted to operate at leading power factor. The same configuration also works with synchronous machines.

All the VSR above described, can also be implemented with three-level converters [46], being the most popular the topology called diode clamped converter, which is shown in Fig. 35. The control strategy is essentially the same already described. This back to back three-phase topology is today the standard solution for high power laminators, which typically demand four quadrants operation [47]. In addition, this solution has been recently introduced in high power downhill conveyor belts which operate almost permanently in the regeneration mode [48].

C. Three-phase PWM Current Source Rectifiers

In commercial ASDs as the one shown in Fig. 36, the CSR has the role of keeping the DC-link current equal to a reference while keeping unity displacement power factor. Normally, an external control loop, based on the speed of the drive, sets it [23], [39]. The commercial units for medium voltage and MW applications use a high performance front end rectifier based on two series connected CSRs, as shown in Fig. 37. The use of a delta/way transformer naturally eliminates the 5th, 7th, 17th, 19th, ..., $6(2q + 1) \pm 1$ current harmonics at the AC mains. This allows the overall topology to comply with the harmonic standards in electrical facilities, an important issue in medium voltage applications. To control the DC-link current, the gating pattern is modulated preferable by means of the SHE technique. Thus, the pattern could eliminate the 11th, 13th, . . . and control the fundamental current component which in turns controls the DC-link current. Additional advantages of this ASD is the natural regeneration capability as the CSRs can reverse the DC-link voltage allowing the sustained power flow from the load into the AC mains. Finally, due to the capacitive filter at the motor side, the motor voltages and consequently the currents become nearly sinusoidal. This reduces the pulsating torques and the currents trough the
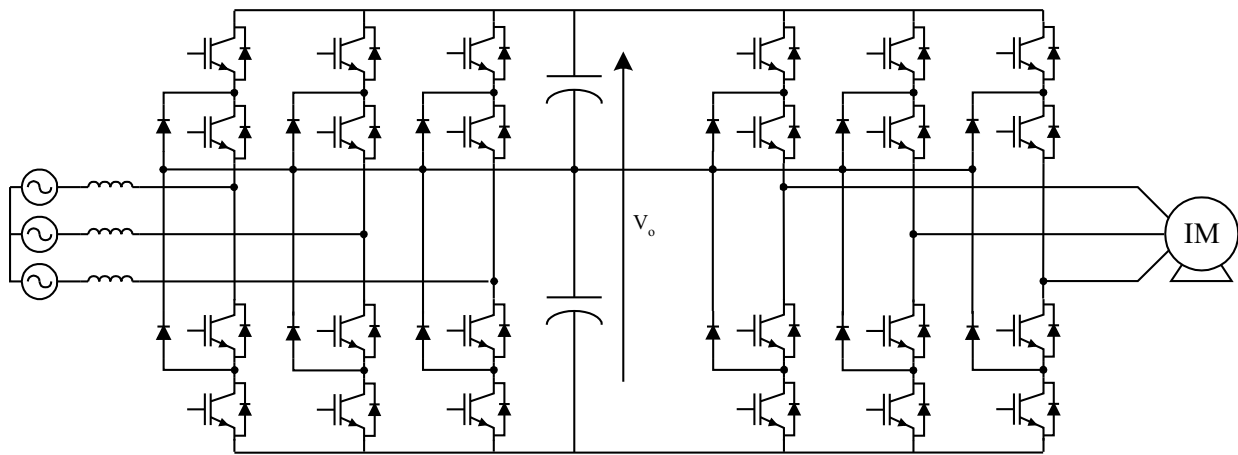
Fig. 35.   Three-level Voltage Source Rectifier feeding a three-level Voltage Source Inverter.
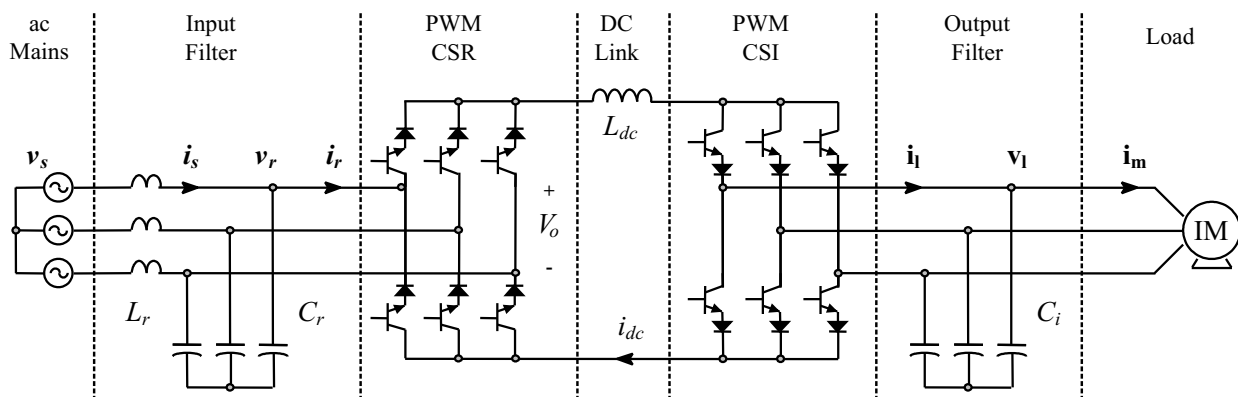

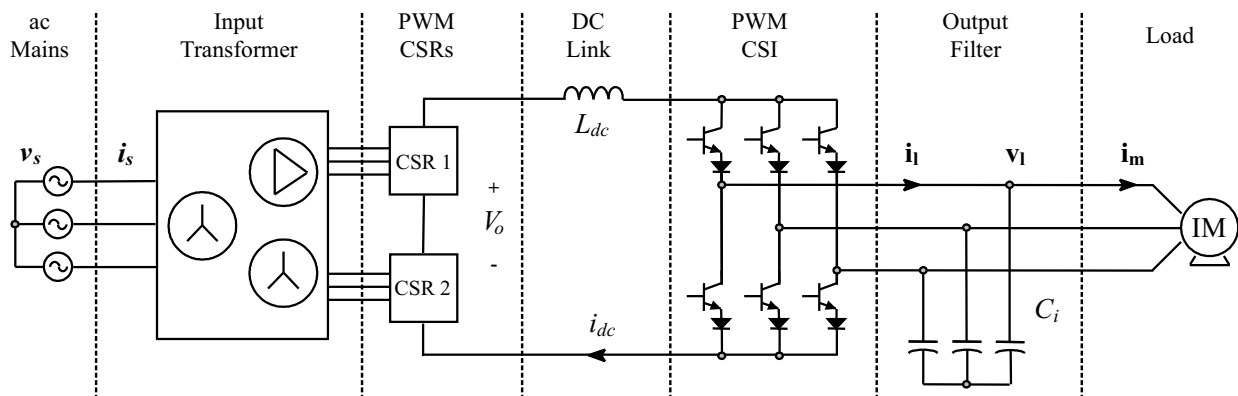Fig. 36.   ASD based on a current source DC-link.

Fig. 37.   High power CSI with two series connected SCR.

neutral. These are two important considerations in medium voltage electrical machines.

V. CONCLUSIONS

This paper has reviewed the most important topologies and control schemes used to obtain AC-DC conversion with bidirectional power flow and very high power factor.

Voltage source PWM regenerative rectifiers have shown a tremendous development from single-phase low power supplies up to high power multilevel units.

Current source PWM regenerative rectifiers are conceptually possible and with few applications in DC motor drives. The main field of application of this topology is the line side converter of medium voltage current source inverters.

Especially relevant is to mention that single-phase PWM regenerative rectifiers are today the standard solution in modern AC locomotives.

The control methods developed for this application allow for an effective control of input and output voltage and currents, minimizing the size of energy storage elements.

This technology has approximately three decades of sustained theoretical and technological development and it can be con-

cluded that these high performance rectifiers comply with modern standards and have been widely accepted in industry.

References

[1] N. Mohan, T. Undeland, W. Robbins, *"Power Electronics: Converters Applications and Design,"* Wiley Text Books, Third Edition, 2002, ISBN: 0471226939.

[2] A. Trzynadlowski *"Introduction to Modern Power Electronics,"* Wiley-Interscience, First Edition, 1998, ISBN: 0471153036.

[3] J. Arrillaga, N. Watson "Power System Harmonics," John Wiley & Sons. Inc, Second Edition, 2003, ISBN: 0470851295.

[4] D. Paice *"Power Electronic Converter Harmonics - Multipulse Methods for Clean Power,"* IEEE Press, Second Edition, 1996, ISBN: 078031137X.

[5] "IEEE 519 Recommended practices and requirements for harmonics control in electrical power systems," *Technichal Report, IEEE Industrial Applications Society/Power Engineering Society*, 1993.

[6] *Limits for Harmonics Current Emissions (Equipment Input Current<16A per Phase)*, IEC 1000-3-2 International Standard, 1995.

[7] *Limits for Harmonic Current Emissions (Equipment Input Current up to and Including 16 A per Phase)*, IEC 61000-3-2 International Standard, 2000.

[8] H. Akagi, Y. Tsukamoto, A. Nabae "Analysis and Design of an Active Power Filter Quad-Series Voltage Source PWM Converters," *IEEE Transactions on Industrial Electronics*, Vol. 26, No 1, pp. 93-98, Feb. 1990.

[9] F. Z. Peng, H. Akagi, A. Nabae "A New Approach to Harmonic Compensation in Power System - A Combines System of Shunt Passive and Series Active Filters," *IEEE Transactions on Industrial Electronics*, Vol. 26, No 6, pp. 983-990, Dec. 1990.

[10] H. Akagi, H. Fujita "New Power Line Conditioner for Harmonic Compensation in Power Systems," *IEEE Transactions on Power Delivery*, Vol. 10, No 3, pp. 1570-1575, Jul. 1995.

[11] B. Singh, B. N. Singh, A. Chandra, K. Al-Hadad, A. Pandey, D. Kothari "A Review of Single-Phase Improved Power Quality AC-DC Converters," *IEEE Transactions on Industrial Electronics*, Vol. 50, No 5, pp. 962-981, Oct. 2003.

[12] O. García, J. Cobos, R. Prieto, P. Alou J. Uceda "Single Phase Power Factor Correction: A Survey," *IEEE Transactions on Power Electronics*, Vol. 18, No 3, pp. 749-755, May 2003.

[13] A. R. Prasad, P. Ziogas, S. Manias "An Active Power Factor Correction Technique for Three-Phase Diode Rectifiers," *IEEE Transactions on Power Electronics*, Vol. 6, No 1, pp. 83-92, Jan. 1991.

[14] J. Kolar, F. Zach "A Novel Three-Phase Utility Interface Minimizing Line Current Harmonics of High-Power Telecomunications Rectifier Modules," *Record of the 16th IEEE International Telecommunications Energy Conference*, Vancouver, Canada, pp. 367-374, Oct. 30-Nov. 3 1994.

[15] J. Kolar, U. Drofenik, F. Zach "Space Vector Based Analysis of the Variation and Control of the Neutral Point Potential of Hysteresis Current Controlled Three-Phase/Switch/Level PWM Rectifier System," *Proceedings of the International Conference on Power Electronics and Drive Systems*, Singapore, Vol. 1, pp.22-33, Feb.21-24 1995.

[16] O. Stihi, B. Ooi "A Single-Phase Controlled-Current PWM Rectifier," *IEEE Transactions on Power Electronics*, Vol. 3, N 4, pp. 453-459, Oct. 1988.

[17] J. Rodríguez, L. Morán, J. Pontt, J. Hernández, L. Silva, C. Silva, P. Lezana "High-Voltage Multilevel Converter With Regeneration Capability," *IEEE Transactions on Industrial Electronics*, Vol. 49, No 4, pp. 839-846, Aug. 2002.

[18] Y. Lo, T. Song, H, Chiu "Analysis and Elimination of Voltage Imbalance Between the Split Capacitors in Half-Bridge Boost Rectifier," *Letters to Editor, IEEE Transaction on Industrial Electronics*, Vol. 49, No 5, Oct. 2002.

[19] J. W. Dixon, "Three-Phase Controlled Rectifiers," *Handbook of Power Electronics*, Chapter 12, M. H. Rashid, Editor in Chief, Academic Press, pp-599-627, 2001.

[20] B. T. Ooi, J. W. Dixon, A. B. Kulkarni, and M. Nishimoto, "An integrated AC Drive System Using a Controlled-Current PWM Rectifier/Inverter Link," *IEEE Transactions on Power Electronics*, Vol. 3, N 1, pp. 64-71, Jan. 1988.

[21] J. W. Dixon and B. T. Ooi, "Indirect Current Control of a Unity Power Factor Sinusoidal Current Boost Type Three-Phase Rectifier," *IEEE Transactions on Industrial Electronics*, Vol. 35, N 4, pp.508-515, Nov. 1988.

[22] M. A. Boost and P. Ziogas, "State-of-the-Art PWM Techniques, a Critical Evaluation," *IEEE Transactions on Industry Applications*, Vol. 24, N 2, pp. 271-280, Mar. 1988.

[23] J. Rodríguez, L. Morán, J. Pontt, R. Osorio and, S. Kouro, "Modeling and Analysis of Common-Mode Voltages Generated in Medium Voltage PWM-CSI Drives," *IEEE Transactions on Power Electronics*, vol. 18, No 3, pp. 873-879, May. 2003.

[24] A. Weber, T. Dalibor, P. Kern, B. Oedegard, J. Waldmeyer, and E. Carroll, "Reverse Blocking IGCTs for Current Source Inverters," *ABB Semiconductors AG* in PCIM 2000.

[25] J. Espinoza and G. Joos. "Current Source Converter On-Line Pattern Generator Switching Frequency Minimization," *IEEE Transactions Industrial Electronics*, vol. 44, No 2, pp. 198-206, Apr. 1997.

[26] H. Karshenas, H. Kojori, and S. Dewan, "Generalized techniques of selective harmonic elimination and current control in current source inverters/converters," *IEEE Transactions on Power Electronics*, vol. 10, No 5, pp. 566-573, Sept. 1995.

[27] D. Sharon, and F.W. Fuchs, "Switched Link PWM Current Source Converters with Harmonic Elimination at the Mains," *IEEE Transactions on Power Electronics*, vol. 15, No 2, pp. 231-241, Mar. 2000.

[28] J. Espinoza, G. Joós, J. Guzmán, L. Morán, and R. Burgos, "Selective harmonic elimination and current/voltage control in current/voltage source topologies: A unified approach," *IEEE Transactions Industrial Electronics*, vol. 48, No 1, pp. 71-81, Feb. 2001.

[29] P. Enjeti, P. Ziogas, and J. Lindsay, "Programmed PWM technique to eliminate harmonics: A critical evaluation," *IEEE Transactions Industrial Applications*, vol. 26, No 2, pp. 302-316, Mar. 1990.

[30] K. Imaie, O. Tsukamoto, and Y. Nagai, "Control Strategies for Multiple Parallel Current-Source Converters of SMES System," *IEEE Transactions on Power Electronics*, vol. 15, No 2, pp. 377-385, March 2000.

[31] J. Guzmán, J. Espinoza, and M. Pérez, "Improved performance of multipulse current and voltage source converters by means of a modified SHE modulation technique," *in Conference Records* IECON'02.

[32] M. Salo and H. Tuusa, "A Vector Controlled Current-Source PWM Rectifier with a Novel Current Damping Method," *IEEE Transactions on Power Electronics*, vol. 15, No 3, pp. 464-470, May. 2000.

[33] B. Han, S. Moon, J. Park, and G. Karady, "Static Synchronous Compensator Using Thyristor PWM Current Source Inverter," *IEEE Transactions on Power Delivery*, vol. 15, No 4, pp. 1285-1290, October 2000.

[34] D. Shen and P.W. Lehn, "Modeling, Analysis, and Control of a Current Source Inverter-Based STATCOM," IEEE Transactions on Power Delivery, vol. 17, No 1, pp. 248-253, Jan. 2002.

[35] Y. Xiao, B. Wu, S. Rizzo, and R. Sotudeh,, "A Novel Power Factor Control Scheme for High-Power GTO Current-Source Converter," *IEEE Transactions on Industry Applications*, vol. 34, No 6, pp. 1278-1283, Dic. 1998.

[36] J. Espinoza and G. Joós, "State variable decoupling and power flow control in PWM current source rectifiers," *IEEE Transactions Industrial Electronics*, vol. 45, No 1, pp. 78-87, Feb. 1998.

[37] M. Salo and H. Tuusa, "A Novel Open-Loop Control Method for a Current-Source Active Power Filter," *IEEE Transactions on Industrial Electronics*, vol. 50, No 2, pp. 313-321, Apr. 2003.

[38] R.E. Shatshat, M. Kazerani, and M. Salama, "Multi Converter Approach to Active Power Filtering Using Current Source Converters," *IEEE Transactions on Power Delivery*, vol. 16, No 1, pp. 38-45, Jan. 2001.

[39] N. Zargari; S. Rizzo; Y. Xiao, H. Iwamoto; K. Satoh, J. Donlon, "A new current-source converter using a symmetric gate-commutated thyristor (SGCT)," *IEEE Transactions on Industry Applications*, vol. 37, No 3, pp. 896 - 903, May-June 2001.

[40] K. Hirachi, H. Yamamoto, T. Matsui, S. Watanabe, M. Nakaoka, "Cost-Effective Practical Developments of High-Performance 1kVA UPS with New System Configurations and their Specific Control Implementations," *European Conference on Power Electronics EPE 95*, Spain 1995, pp. 2035-2040.

[41] K. Hückelheim, Ch. Mangold, "Novel 4-Quadrant Converter Control Method," *European Conference on Power Electronics EPE 89*, Germany 1989, pp. 573-576.

[42] T. Ohmae, K. Nakamura, "Hitachi's Role in the Area of Power Electronics for Transportation," *Proceedings of the IECON'93*. Hawai, pp. 714-718, Nov. 1993.

[43] P. Enjeti, A. Rahman "A New Single-Phase to Three-Phase Converter with Active Input Current Shaping for Low Cost AC Motor Drives," *IEEE Transactions on Industry Applications*, Vol. 29, No 4., pp. 806-813, Aug 1993.

[44] C. Jacobina, M. Beltrao, E. Cabral, A. Nogueira, "Induction Motor Drive System for Low-Power Applications," *IEEE Transactions on Industry Applications*, Vol. 35, No 1. pp. 52-60, Jan/Feb 1999.

[45] T. Uematsu, T. Ikeda, N. Hirao, S, Totsuka, T. Ninomiya, H. Kawamoto "A Study of the High Performance Single Phase UPS," *Record of the 29th Annual IEEE Power Electronics Specialists Conference, PESC'98*, Fukuoka, Japan, pp. 1872-1878.

[46] A. Draou, M. Benghanem and A. Tahri, "Multilevel Converters and VAR Compensation," Chapter 25, *Handbook of Power Electronics*, M. H. Rashid, Editor in Chief, Academic Press, pp-599-627, 2001.

[47] M. Koyama, Y. Shimomura, H. Yamaguchi, M. Mukunoki, H. Okayama and S. Mizoguchi, "Large capacity High Efficiency Three-Level GCT Inverter System for Steel Rolling Mill Drivers," *Proceedings of the 9th European Conference on Power Electronics*, EPE 2001, Austria, CD-ROM.

[48] J. Rodríguez, J. Pontt, N. Becker, A. Weinstein, "Regenerative Drivers in the Megawatt Range for High-Performance Downhill Conveyors," *IEEE Transactions on Industry Applications*, Vol. 38, No 1, pp. 203-210, Jan/Feb 2002.

José Rodríguez

PLACE
PHOTO
HERE

Juan Dixon

PLACE
PHOTO
HERE

José Espinoza

PLACE
PHOTO
HERE

Pablo Lezana

PLACE
PHOTO
HERE